200 determined by the bubble flow meter (Gilibrator-2) with a relative accuracy being less
201 than 1%. The uncertainty of the IUCPC was calculated to be about 10%. Detailed
202 uncertainty analysis can be found in another paper (Chen et al., 2016). Before the
203 counting efficiency measurement, the TSI 3775 was connected to the DMA
204 essentially working as a scanning mobility particles sizer (SMPS) to ensure stable
205 particle generation from the burner or the ambient air. Throughout the experiments,
206 homogeneous nucleation (self-condensation of working liquid) was absent, because
207 not a single particle was detected after five-minute counting when the in-house CPC
208 was challenged with HEPA filtered gas.

209 A separate experiment was carried out to analyze the morphology of CH_4 and
210 C_2H_4 combustion particles, which may provide some insight into how the counting
211 efficiency of IUCPC is influenced by the micro-structure of challenging particles.
212 TEM images are obtained through a JEM-2100F electron microscope operating at 200
213 kV using LaB6 filament. The TEM sample was created by dispersing a portion of the
214 collected material from the filter upon TEM grids (400 mesh Copper, Electron
215 Microscopy Sciences).

216

217 ## RESULTS AND DISCUSSION

218 ***TEM images of combustion particles***

219 The TEM images of the combustion product of CH_4 and C_2H_4 are presented in

figure 3 and figure 4 respectively. The morphology of ambient particles are not presented because of its scarcity and great variation. Most of the CH_4 and C_2H_4 combustion particles are considered as sphere while a small proportion of the combustion particles have a wavy edge. Compared with CH_4 combustion particles, C_2H_4 combustion particles seem to be deviate more from spherical shape. In addition, the agglomerates of C_2H_4 primary particles are more branched and less spherical than the agglomerates of CH_4 primary particles, which means that C_2H_4 particles have larger contact area with the working fluid and thus could be more easily activated in the CPC condenser. The different grayscale and fringe pattern of primary particles from different sources imply that CH_4 and C_2H_4 may generate particles of different chemical compositions.

Experimental counting efficiencies

Fig. 5 shows the experimental results at T_s=38 ℃ and T_c=29 ℃ when the IUCPC was challenged with CH_4 and C_2H_4 particles. The counting efficiency increased from 0 to 1 for both CH_4 and C_2H_4 particles as the particle size increased from 13 nm to 19 nm, and C_2H_4 combustion particles exhibited a higher counting efficiency at the same particle size. A plausible reason for the difference of the counting efficiency between CH_4 combustion particles and C_2H_4 combustion particles could be the differences in their hygroscopic properties. The hygroscopic properties of test particles to the working fluid are normally influenced by two factors, namely the composition of test particles and the morphology of the particles. Since particles are

241 not exposed to a high humidity environment before entering the condenser for the
242 sheath flow type CPC, they need to be activated within the period of the time in the
243 condenser, and thus the activation is more easily influenced by the hygroscopic
244 properties of the test particles compared to a full flow type CPC. In general, particles
245 featuring a higher hygroscopic property to the working fluid are more likely to be
246 activated in the condenser.

247 The difference in the composition of the CH_4 combustion particles and C_2H_4
248 combustion particles may influence the wettability of the two types of particles with
249 butanol, and thus influence the counting efficiency curve. C_2H_4 is considered to
250 generate more carbonaceous particles than CH_4 because C_2H_4 could form PAHs
251 (Poly-Aromatic Hydrocarbons) relatively easily, which are the soot precursor (Shukla
252 and Koshi, 2012).

253 The shape of test particles may be another reason contributing to the counting
254 efficiency difference. Compared with ideal spherical particles, non-spherical particles
255 experience higher drag in a differential mobility analyser (DMA), and this will lead to
256 a slight overestimation of their physical size based on their electrical mobility. On the
257 other hand, non-spherical particles may have more contacting line with the working
258 fluid, and thus have higher wettability to the n-butanol. Fig. 6 demonstrates that the
259 experimental counting efficiencies with the temperature difference of 9 ℃ for both
260 conditions T_s=31 ℃, T_c=22 ℃ and T_s=36 ℃, T_c=27 ℃. The former case showed
261 a higher overall counting efficiency, which may be due to the non-linear relationship

between the saturation pressure of butanol and the temperature. When the temperature difference reduced from 9 ℃ to 6 ℃, the D_0 (the particle size with which the counting efficiency is just above 0) and D_{50} (cut-off diameter) increased from 12.2 nm, 13.6 nm to 14.8 nm, 17.9 nm, respectively. When the temperature difference was further reduced, the D_{50} increased significantly and was much larger than 23 nm. The results were not shown here because such large cut-off sizes are rarely found in the real applications of CPCs.

Table 1 listed the cut-off size (D_{50}) and the lowest detectable size (D_0) of the IUCPC operating at several working conditions when it is challenged with different particle sources. When the temperature difference of the saturator and the condenser was set to be 9℃, the cut-off size of IUCPC can be found to be more sensitive to the change of the challenging particles as well as the average temperature of the saturator and condenser than the lowest detectable size. The wettability of the ambient particles to working fluid was thought to rank between that of CH_4 combustion particles and C_2H_4 combustion particles.

Conclusion

A sheath type CPC has been constructed to investigate the factors influencing the counting efficiency when challenged with particles from a Bunsen burner and ambient air. The experiments demonstrated that the counting efficiency is closely linked to the combination of the saturator temperature and the condenser temperature, and to the

contact angle, which is an indicator of the wettability (or affinity) between particles and the working fluid. When the temperature difference between the saturator and condenser remains constant, the counting efficiency curve of the in-house CPC challenged by ambient particles moved toward left as the average saturator and condenser temperature decreased.

ACKNOWLEDGEMENT

This research is supported by National Natural Science Foundation of China (91641119 and 41575119). This project is also supported by special fund of State Key Joint Laboratory of Environment Simulation and Pollution Control (Grant No. 17K03ESPCP).

REFERENCES

Agarwal, J.K. and Sem, G.J. (1980). Continuous flow, single-particle-counting condensation nucleus counter. *J. Aerosol Sci* 11: 343-357.

Aitken, J. (1881). Xii.—on dust, fogs, and clouds. *Transactions of the Royal Society of Edinburgh* 30: 337-368.

Amara, A.B., Dauphin, R., Babiker, H., Viollet, Y., Chang, J., Jeuland, N. and Amer, A. (2016). Revisiting diesel fuel formulation from petroleum light and middle refinery streams based on optimized engine behavior. *Fuel* 174: 63-75.

Biswas, S., Fine, P.M., Geller, M.D., Hering, S.V. and Sioutas, C. (2005). Performance evaluation of a recently developed water-based condensation particle counter. *Aerosol Sci. Technol.* 39: 419-427.

Chen, L., Liang, Z., Zhang, X. and Shuai, S. (2017). Characterizing particulate matter emissions from gdi and pfi vehicles under transient and cold start conditions. *Fuel* 189: 131-140.

Chen, L., Ma, Y., Guo, Y., Zhang, C., Liang, Z. and Zhang, X. (2016). Quantifying the effects of operational parameters on the counting efficiency of a condensation particle counter using response surface design of experiments (doe). *J. Aerosol Sci*.

Chen, L., Stone, R. and Richardson, D. (2012a). Effect of the valve timing and the coolant temperature on particulate emissions from a gasoline direct-injection engine fuelled with gasoline and with a gasoline–ethanol blend. *Proc. Inst. Mech. Eng. Part D-J. Automob. Eng.* 226: 1419-1430.

Chen, L., Stone, R. and Richardson, D. (2012b). A study of mixture preparation and pm emissions using a direct injection engine fuelled with stoichiometric gasoline/ethanol blends. *Fuel* 96: 120-130.

Chen, L., Zhang, Z., Gong, W. and Liang, Z. (2015). Quantifying the effects of fuel compositions on gdi-derived particle emissions using the optimal mixture design of experiments. *Fuel* 154: 252-260.

Collings, N., Rongchai, K. and Symonds, J.P.R. (2014). A condensation particle counter insensitive to volatile particles. *J. Aerosol Sci* 73: 27-38.

Coulier, P.-J. (1875). Note on a new property of the air. *Journal of Pharmacy and Chemistry* 22: 165-173.

Espy, J.P. (1841). *The philosophy of storms*. CC Little and J. Brown.

Fletcher, N.H. (1958). Size effect in heterogeneous nucleation. *J. Chem. Phys.* 29: 572.

Giakoumis, E.G., Rakopoulos, C.D., Dimaratos, A.M. and Rakopoulos, D.C. (2012). Exhaust emissions of diesel engines operating under transient conditions with biodiesel fuel blends. *Prog. Energy Combust. Sci.* 38: 691-715.

Giechaskiel, B. and Bergmann, A. (2011). Validation of 14 used, re-calibrated and new tsi 3790 condensation particle counters according to the un-ece regulation 83. *J. Aerosol Sci* 42: 195-203.

Giechaskiel, B., Wang, X., Gilliland, D. and Drossinos, Y. (2011). The effect of particle chemical composition on the activation probability in n-butanol condensation particle counters. *J. Aerosol Sci* 42: 20-37.

Hakala, J., Manninen, H.E., Petäjä, T. and Sipilä, M. (2013). Counting efficiency of a tsi environmental particle counter monitor model 3783. *Aerosol Sci. Technol.* 47: 482-487.

Hering, S.V., Stolzenburg, M.R., Quant, F.R., Oberreit, D.R. and Keady, P.B. (2005). A laminar-flow, water-based condensation particle counter (wcpc). *Aerosol Sci. Technol.* 39: 659-672.

Hermann, M. and Wiedensohler, A. (2001). Counting efficiency of condensation particle counters at low-pressures with illustrative data from the upper troposphere. *J. Aerosol Sci* 32: 975-991.

Hoppel, W., Twomey, S. and Wojciechowski, T. (1979). A segmented thermal diffusion chamber for continuous measurements of cn. *J. Aerosol Sci* 10: 369-373.

Iida, K., Stolzenburg, M.R. and McMurry, P.H. (2009). Effect of working fluid on sub-2 nm particle detection with a laminar flow ultrafine condensation particle counter. *Aerosol Sci. Technol.* 43: 81-96.

Iida, K., Stolzenburg, M.R., McMurry, P.H., Smith, J.N., Quant, F.R., Oberreit, D.R., Keady, P.B., Eiguren-Fernandez, A., Lewis, G.S., Kreisberg, N.M. and Hering, S.V. (2008). An ultrafine, water-based condensation particle counter and its evaluation under field conditions. *Aerosol Sci. Technol.* 42: 862-871.

Jiang, J., Attoui, M., Heim, M., Brunelli, N.A., McMurry, P.H., Kasper, G., Flagan, R.C., Giapis, K. and Mouret, G. (2011). Transfer functions and penetrations of five differential mobility analyzers for sub-2 nm particle classification. *Aerosol Sci. Technol.* 45: 480-492.

Kousaka, Y., Niida, T., Okuyama, K. and Tanaka, H. (1982). Development of a mixing type condensation nucleus counter. *J. Aerosol Sci* 13: 231-240.

Kulmala, M., Mordas, G., Petäjä, T., Grönholm, T., Aalto, P.P., Vehkamäki, H., Hienola, A.I., Herrmann,

E., Sipilä, M., Riipinen, I., Manninen, H.E., Hämeri, K., Stratmann, F., Bilde, M., Winkler, P.M., Birmili, W. and Wagner, P.E. (2007). The condensation particle counter battery (cpcb): A new tool to investigate the activation properties of nanoparticles. *J. Aerosol Sci* 38: 289-304.

Lee, D.-W., Hopke, P.K., Rasmussen, D.H., Wang, H.-C. and Mavliev, R. (2003). Comparison of experimental and theoretical heterogeneous nucleation on ultrafine carbon particles. *J. Phys. Chem. B* 107: 13813-13822.

Lee, H. and Jeong, Y. (2012). The effect of dynamic operating conditions on nano-particle emissions from a light-duty diesel engine applicable to prime and auxiliary machines on marine vessels. *International Journal of Naval Architecture and Ocean Engineering* 4: 403-411.

Lee, S., Kwak, J., Lee, S. and Lee, J. (2015). On-road chasing and laboratory measurements of exhaust particle emissions of diesel vehicles equipped with aftertreatment technologies (dpf, urea-scr). *Int. J. Nav. Archit. Ocean Eng.* 16: 551-559.

Liu, W., Kaufman, S.L., Osmondson, B.L., Sem, G.J., Quant, F.R. and Oberreit, D.R. (2006). Water-based condensation particle counters for environmental monitoring of ultrafine particles. *J. Air Waste Manage. Assoc.* 56: 444-455.

Mamakos, A., Giechaskiel, B. and Drossinos, Y. (2013a). Experimental and theoretical investigations of the effect of the calibration aerosol material on the counting efficiencies of tsi 3790 condensation particle counters. *Aerosol Sci. Technol.* 47: 11-21.

Mamakos, A., Martini, G. and Manfredi, U. (2013b). Assessment of the legislated particle number measurement procedure for a euro 5 and a euro 6 compliant diesel passenger cars under regulated and unregulated conditions. *J. Aerosol Sci* 55: 31-47.

Mertes, S., Schröder, F. and Wiedensohler, A. (1995). The particle detection efficiency curve of the tsi-3010 cpc as a function of the temperature difference between saturator and condenser. *Aerosol Sci. Technol.* 23: 257-261.

Millo, F., Vezza, D.S., Vlachos, T., De Filippo, A., Ciaravino, C., Russo, N. and Fino, D. (2012). Particle number and size emissions from a small displacement automotive diesel engine: Bioderived vs conventional fossil fuels. *Ind. Eng. Chem. Res.* 51: 7565-7572.

Otsuki, Y., Takeda, K., Haruta, K. and Mori, N. (2014). A solid particle number measurement system including nanoparticles smaller than 23 nanometers. 1.

Petäjä, T., Mordas, G., Manninen, H., Aalto, P.P., Hämeri, K. and Kulmala, M. (2006). Detection efficiency of a water-based tsi condensation particle counter 3785. *Aerosol Sci. Technol.* 40: 1090-1097.

Rongchai, K. (2014). The high temperature condensation particle counter (ht-cpc)–a new instrument for the measurement of solid particulate matter, Ph. D. thesis, University of Cambridge, Department of Engineering.

Sem, G.J. (2002). Design and performance characteristics of three continuous-flow condensation particle counters: A summary. *AtmRe* 62: 267-294.

Shukla, B. and Koshi, M. (2012). A novel route for pah growth in haca based mechanisms. *Combust. Flame* 159: 3589-3596.

Stolzenburg, M.R. and McMurry, P.H. (1991). An ultrafine aerosol condensation nucleus counter. *Aerosol Sci. Technol.* 14: 48-65.

Tan, P.-q., Ruan, S.-s., Hu, Z.-y., Lou, D.-m. and Li, H. (2014). Particle number emissions from a

light-duty diesel engine with biodiesel fuels under transient-state operating conditions. *ApEn* 113: 22-31.

Wilson, J., Hyun, J. and Blackshear, E. (1983). The function and response of an improved stratospheric condensation nucleus counter. *J. Geophys. Res.-Oceans* 88: 6781-6785.

Winkler, P.M., Vrtala, A. and Wagner, P.E. (2008). Condensation particle counting below 2 nm seed particle diameter and the transition from heterogeneous to homogeneous nucleation. *AtmRe* 90: 125-131.

Figure Captions

Fig. 1. The schematic diagram of the laminar flow cooling type CPC

Fig. 2. The schematic of the experimental set-up

Fig. 3. TEM image of CH_4 combustion particles

Fig. 4. TEM image of C_2H_4 combustion particles

Fig. 5. Experimental counting efficiencies at $\mathbf{T_s}$=38 ℃ and $\mathbf{T_c}$=29 ℃. Symbols represent the experimental data of CH_4 particles (circle) and C_2H_4 particles (pentagram).

Fig. 6. Experimental (symbols) results of the in-house CPC challenged with ambient air particles at different combinations of the saturator temperature and the condenser temperature.

Table. 1. Cut-off diameter (D_{50}) and the lowest observable particles (D_0) for CH_4 , C_2H_4 combustion particles and ambient particles when the IUCPC operating at different combinations of saturator and condenser temperatures

418 Table 1

Operating Conditions	Particle source	D_{50}	D_0
T_s=38℃ T_c=29℃	CH_4 combustion particles	16.1	13.5
T_s=38℃ T_c=29℃	C_2H_4 combustion particles	14.1	12.5
T_s=36℃ T_c=27℃	Ambient particles	15.2	12.6
T_s=31℃ T_c=22℃	Ambient particles	13.6	12.2
T_s=31℃ T_c=25℃	Ambient particles	17.9	14.8

419

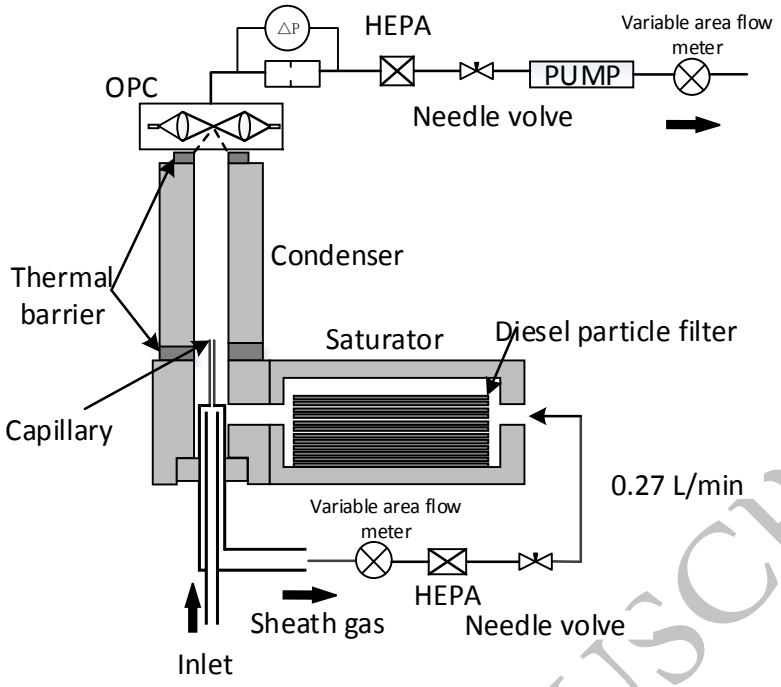

420

421 **Fig. 1**

422

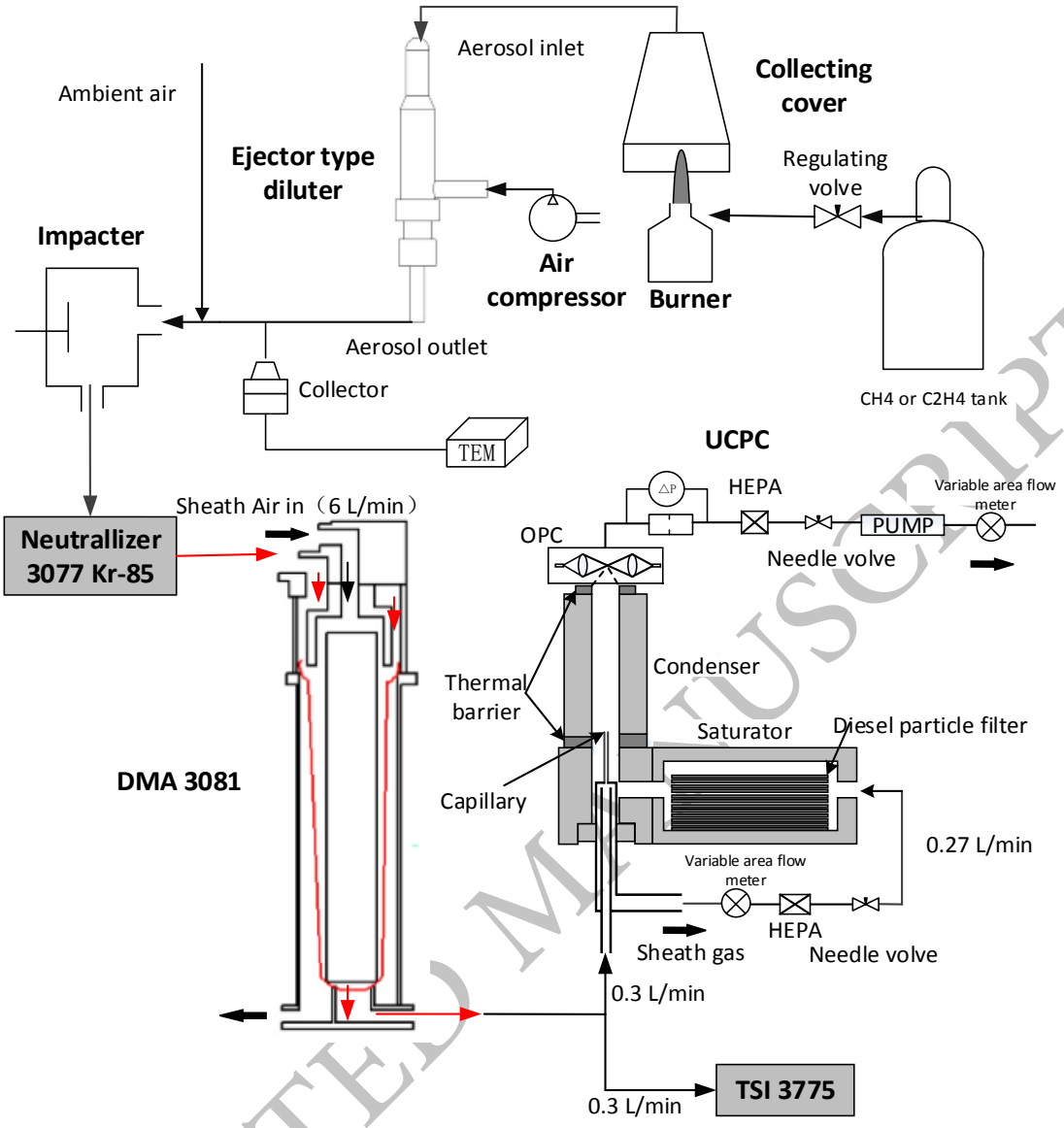

423

424 **Fig. 2**

425

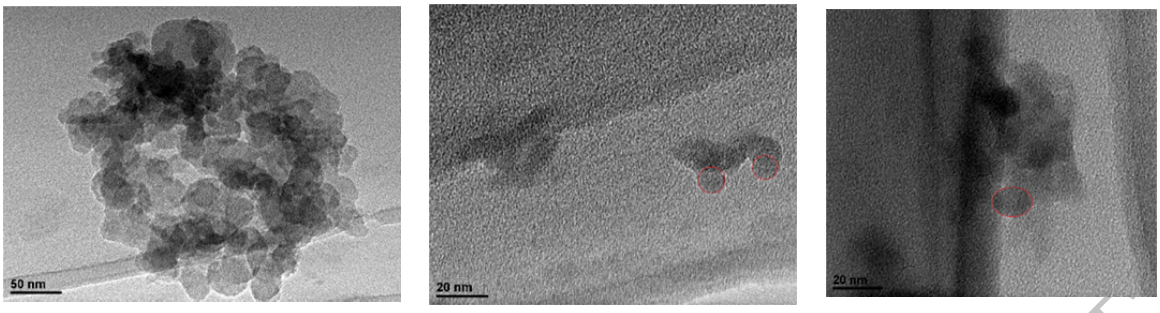

426 **Fig. 3**

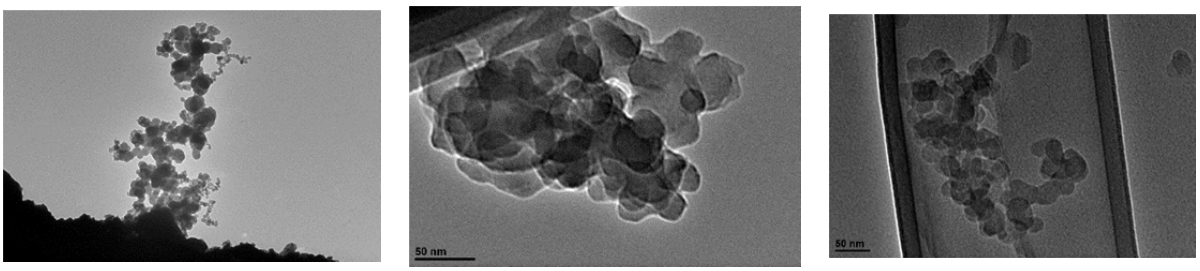

427 **Fig. 4**

428

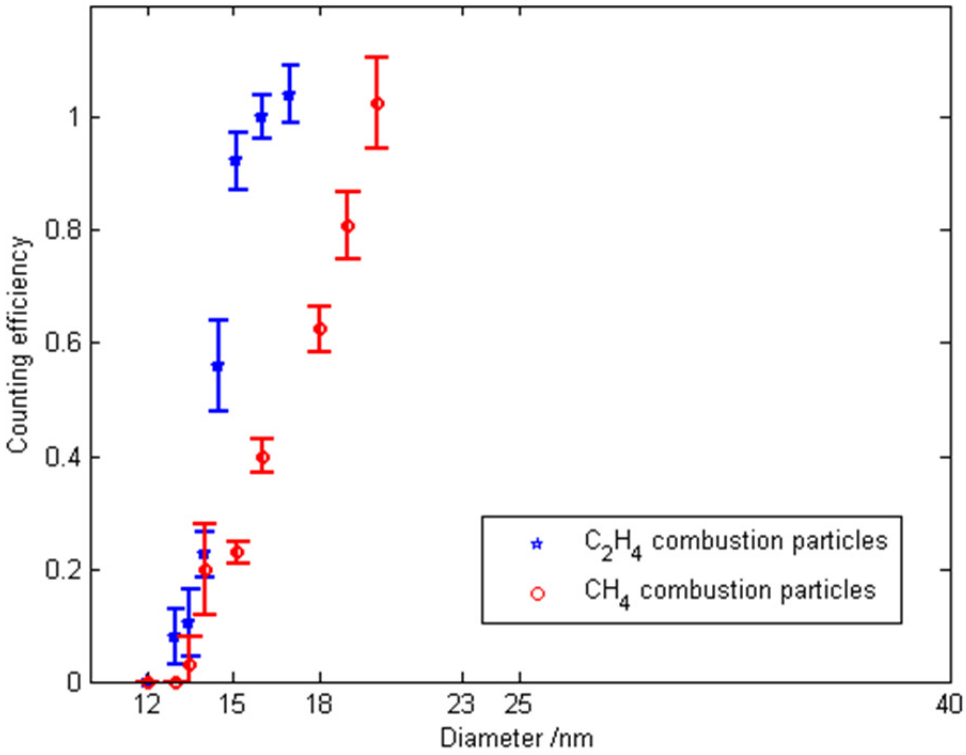

429

430 **Fig. 5**

431

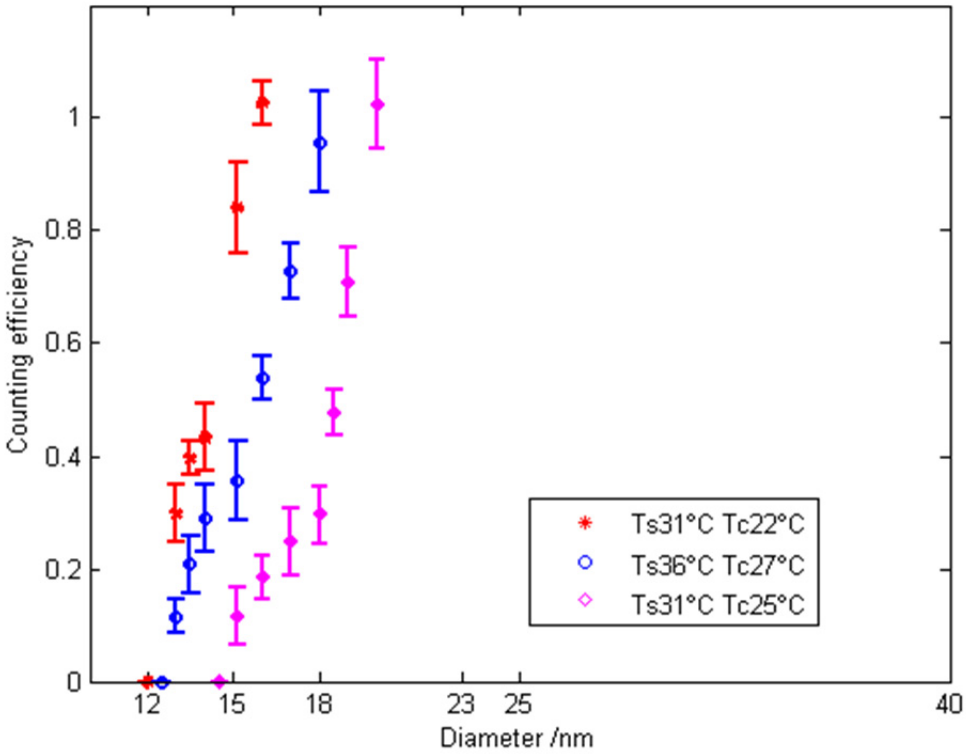

432

433 **Fig. 6**